Comparison of Mean and Peak Pressure Coefficient for Cross-Plan-Shaped Tall Buildings Under Wind

Debasish Kumar and **Sujit Kumar Dalui**

1 Introduction

With the advent of construction technology and scarcity of land, the high-rise building construction is increasing rapidly in important cities. It becomes a challenging role for designers to design tall buildings in the wind environment. Different international codes like IS: 875 (Part-3):2015 [1], AS-NZS: 1180:2002 [2], ASCE-7-10 [3], etc. are available for the design of regular and conventional tall buildings. Nowadays, building shapes are smell out from these conventional shapes instead becoming more irregular and unconventional in plan and elevation. Wind tunnel testing is a very suitable method for such kinds of buildings. With the development of modern computational techniques, CFD becomes a reliable method to deal with those building models.

Gomes et al. [4] investigated L- and U-shaped model wind-induced responses with a 1:100 length scale using an experimental and numerical approach. Bhattacharyya and Dalui [5] investigated an 'E' plan-shaped building to evaluate the mean pressure coefficient, pressure distribution and pressure contours for various wind flow directions and the results showed good agreement between numerical and experimental techniques. A detailed comparison of pressure coefficients and force coefficients for different cross-plan-shaped buildings was conducted by Kumar and Dalui [6] by CFD simulation using ANSYS CFX. A study of '+' plan-shaped tall building models for 0° and 45° wind flow was demonstrated by Chakraborty et al. [7]. Mukherjee et al. [8] conducted a study to evaluate wind pressure variation on 'Y' plan-shaped tall buildings under various wind flow directions through wind tunnel testing. The wind-induced responses of different irregular plan-shaped building like Z-type [9], Y-type [8, 10], C-type [11] and L-type [12] were studied. Li et al. [13] experimentally investigated aerodynamic treatment to reduce wind forces on four

D. Kumar (✉) · S. K. Dalui
Indian Institute of Engineering Science and Technology, Shibpur, Howrah 711201, India

different models. Lui et al. [14] studied the mean, fluctuating and peak wall pressure coefficient for the rectangular tall high-rise building for various plan ratios. Amin and Ahuja [15] pointed out that wind pressure on windward faces is independent of the side ratio for rectangular plan-shaped tall buildings, while the side ratio of such buildings significantly influences wind pressure of side and leeward faces.

Moreover, CFD offers more flexibility for the designer to choose any ground-surface conditions, any approaching wind flow situations, building configurations and various surrounding building arrangements. Different research work was performed to understand the flaws and strength of various influential parameters like appropriate grid size, turbulence profiles, velocity profiles, etc. [16]. Thordal et al. [17] focussed on the essential aspects of atmospheric boundary layer wind flow simulation for numerical approach.

2   Objectives

This paper investigates the comprehensive study of mean and peak pressure coefficient over different surfaces for two cross-plan-shaped tall buildings at various wind flow directions ranging from 0° to 180° at an interval of 30°. Here, one regular cross-plan-shaped tall building is considered a basic model, and angular cross-plan-shaped tall buildings are formed by shifting the limb position by 15°. The overall plan area of these two buildings remains the same. However, the total angle between each limb, i.e. $\alpha_1 + \alpha_2 = 180°$, should be satisfied. To keep the plan area remains the same, and the length of the limbs for the angular cross-plan-shaped model is required to be increased marginally. The detailed dimension of the two building models is shown in Fig. 1a, b.

The regular cross-plan-shaped model prototype dimensions are 30 m in length, 15 m in width and 150 m in height, respectively. The building models are scaled down to a scale of 1:300. The overall plan area of the model is 22500 mm^2. The mean pressure coefficient at each face is derived for both models. Furthermore, peak pressure and power spectral density plot of pressure are also evaluated for both models and compared to comprehend the cross-sectional variation.

3   Numerical Analysis

Computational fluid dynamics (CFD) are proficiently developed boundary layer wind profiles around the building, and the wind-induced responses on and around the building can be evaluated. Here, the ANSYS CFX package is used for numerical simulation. There are various turbulence models available for numerical simulation, such as k-ε model, k-ω model and SST model. Generally, the k-ε model predicts better results for medium turbulence conditions and Chakraborty et al. [7] and Mukherjee et al. [8] used k-ε turbulence model in their numerical study. Thus, the k-ε model is
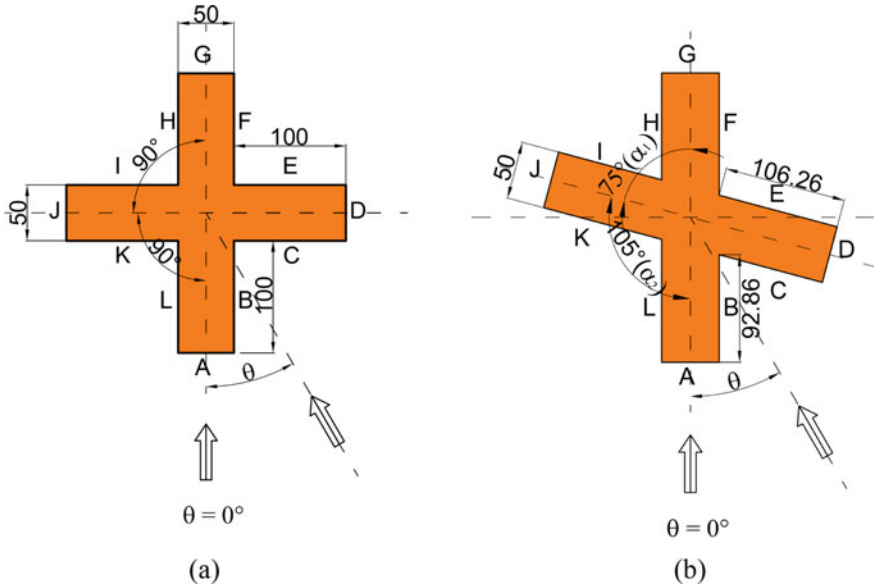
Fig. 1 Typical layout of the regular and angular cross-plan-shaped tall building models with dimensions and face notations

opted here for the present simulation. Furthermore, a comparison is made between the numerical analysis (using the ANSYS CFX package) and Chakraborty et al. [7] results. The dimensional parameter and wind flow parameters related to wind flow are kept similar.

3.1 Velocity Profiles and Meshing Information

To fully incorporate the vortex generations and velocity fluctuations in the wake region of the building [18], upstream, downstream, side clearances and top clearance are 5H, 15H, 5H and 5H, respectively. H is the overall height of the building (shown in Fig. 2a, b). No-slip condition is considered at the building surfaces to obtain the pressure contour. Thus, there is no relative movement between building surfaces and the wind flow layer. The free slip condition is maintained at the domain side and top surfaces. At the interface between wind flow and sidewalls, the velocity field's normal component is zero, but the tangential component is unrestricted. The tangential force is zero. The velocity scale is 1:5 and the velocity at the inlet is 10 m/s. Here, the power law is used with a power index of 0.133 to generate boundary layer wind flow at the domain inlet. A comparison of the velocity profile between numerical simulation and experimental data used by Chakraborty et al. [7] is shown in Fig. 3 and found to be within the acceptable range. The equation of power law is noted
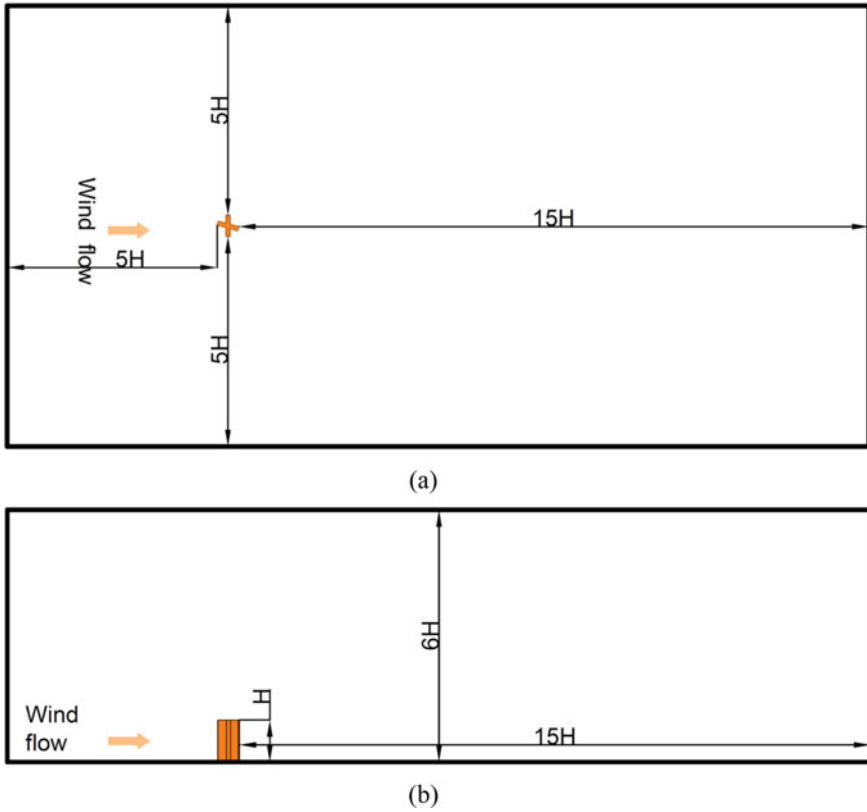
(a)

(b)

Fig. 2 The domain around the building. **a** Plan. **b** Side elevation

below as:

$$\frac{U}{U_o} = \left(\frac{z}{z_o}\right)^{\alpha} \tag{1}$$

where U_o is the basic wind speed taken as 10 m/s,

Z_o is boundary layer height scaled down to 1 m and

α is power index taken as 0.133.

Velocity in other directions is zero. Moreover, a combination of hexagonal and tetrahedral meshing is chosen for meshing the building surface and the rest of the domain. To accurately access the actual pressure fluctuations on the building surfaces, finer meshing is generated. In contrast, the coarse mesh is judicially chosen for the rest of the domain to reduce the time of calculation without losing the accuracy of the obtained results.

Fig. 3 Velocity profile along with height
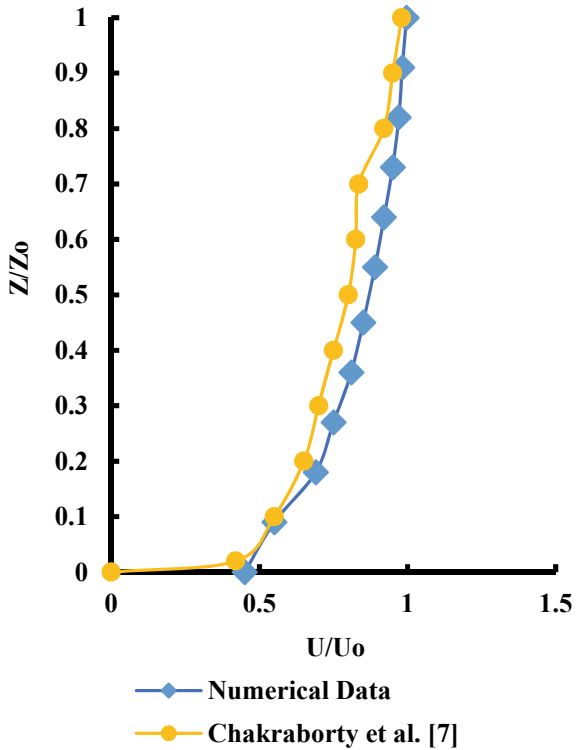
4 Comparison of Numerical Analysis with Experimental Data

The results obtained from numerical analysis using the ANSYS CFX package should be validated with experimental data. The wind tunnel test setup used by Chakraborty et al. [7] and model details of the '+' plan-shaped building were summarized here.

A blower fan of 125HP is used to generate a continuous flow of wind through the wind tunnel, having a cross-section of 2 m (width) × 2 m (height) and a length of 38 m. A 6 m (width) and 6 m (depth) square-holed honeycomb wire mesh is located at the wind tunnel entrance to generate a streamline of flow with a very mild velocity with less turbulence. An elliptical effuse profile of 6 m in length with a contraction ratio of 9:5:1 is used to increase wind flow velocity. The wind must pass through the vortex generator and barrier wall to simulate a small desired and controlled degree of turbulence in the wind velocity. The experiments are conducted considering terrain category-II, which corresponds to open terrain with well-scattered obstructions having heights generally between 1.5 and 10 m, as per IS 875 (Part-III):2015. Square cubes of different sizes are positioned on the wind tunnel upstream side. A dyno drive is attached with a diffuser or fan at the outlet to control wind flow velocity. A pitot tube is attached to the wind tunnel at a distance of 7.8 m from

the elliptical effuse to measure wind velocity in the wind tunnel and reference point. The wind tunnel is also mechanized with a hot-wire anemometer and a manometer. A pressure transducer is connected with the pressure tapping point and the reference pressure point to measure the pressure through Barron instruments. The Perspex sheet is generally used for a pressure measurement model having a thickness of 4 mm. Pressure points are installed on surfaces of the models with suitable spacing, both along with height and width, to predict pressure fluctuation on the surface and the edges more precisely. The pressure tapings are made of stainless steel tubes with 1 mm internal diameter and 15–20 mm-long, placed flush with the mode surfaces by drilling holes at each grid point.

The mean pressure coefficients for different faces evaluated from the numerical analysis are compared with the experimental results by Chakraborty et al. [7] at 0° wind flow direction which is represented in Fig. 6. The dimensional parameter and wind flow parameters are maintained analogous for these two cases. Marginal deviations are noted on the few selected faces like Face A and Face K, but discrepancies are within the acceptable limits. These differences are due to the insufficiency of pressure tapping points on the surfaces and edges to acquire pressure fluctuations in experimental analysis. It has been observed that the numerical result is slightly higher than the experimental results but within the acceptable range.

5   Results and Discussions

5.1   Mean Pressure Coefficients (C_p)

The mean pressure coefficients on different surfaces for both building models at 0°, 30°, 60° and 90° wind incidence angles are depicted in Table 1. For the regular cross-plan-shaped model, the maximum positive mean C_p at Face A is observed for 0° wind incidence angle and maximum suction depicted for 60° angle of attack. The mean C_p is reduced at Face A for the angular building model at 0° wind flow. The most unfavourable mean negative C_p is observed at Face D for regular cross-plan-shaped building at 30° angle of attack due to a larger separation of flow. A maximum positive mean C_p is depicted at Face B for angular cross-plan-shaped buildings at 30° wind flow due to the combined effect of mutual interference and the larger frontal surface facing the approaching wind directly. Moderate suction is prevailing in the side and leeward faces of both building models.

5.2   Peak Pressure Coefficients ($\widehat{C_p}$)

The peak pressure coefficients at each face for both cross-plan-shaped building models at 0° wind incidence angle are represented in Fig. 4. The peak pressure

Table 1 Pressure coefficient on different surfaces of regular and angular cross-plan-shaped tall buildings at 0°, 30°, 60° and 90° wind incidence angles

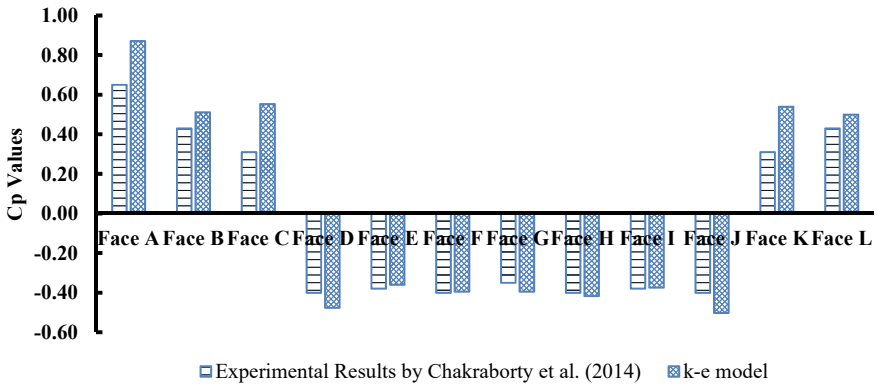| Faces	Mean pressure coefficients							
	0° wind flow		30° wind flow		60° wind flow		90° wind flow	
	Regular	Angular	Regular	Angular	Regular	Angular	Regular	Angular
Face A	0.871	0.855	0.222	0.324	−0.819	−0.627	−0.505	−0.543
Face B	0.511	0.630	0.914	0.919	0.784	0.796	0.540	0.206
Face C	0.553	0.654	0.783	0.872	0.917	0.896	0.503	0.113
Face D	−0.476	−0.478	−0.858	−0.311	0.226	0.625	0.869	0.754
Face E	−0.360	−0.349	−0.557	−0.574	−0.665	−0.276	0.506	0.821
Face F	−0.395	−0.406	−0.550	−0.542	−0.468	−0.125	0.540	0.702
Face G	−0.396	−0.372	−0.451	−0.406	−0.455	−0.413	−0.515	−0.455
Face H	−0.417	−0.371	−0.395	−0.347	−0.367	−0.327	−0.369	−0.395
Face I	−0.374	−0.346	−0.378	−0.333	−0.384	−0.351	−0.405	−0.427
Face J	−0.503	−0.447	−0.466	−0.412	−0.448	−0.368	−0.398	−0.396
Face K	0.539	0.424	−0.466	−0.547	−0.546	−0.433	−0.415	−0.506
Face L	0.500	0.234	−0.663	−0.713	−0.547	−0.391	−0.371	−0.448

Fig. 4 Comparison of mean pressure coefficients on different surface of building for regular cross-plan-shaped building model at 0° wind incidence angle for numerical and experimental results by Chakraborty et al. [7]

coefficients are higher than the mean pressure coefficients, and these differences are noticed mainly at the top, bottom and edges of the building surfaces. The difference between the $\widehat{C_p}$ and C_p is mainly attributed to the existence of body-generated turbulence and normalization of 3-s gust speed to obtain peak pressure value. The peak pressure coefficients are obtained by measured instantaneous pressure normalized over 3-s gust speed.
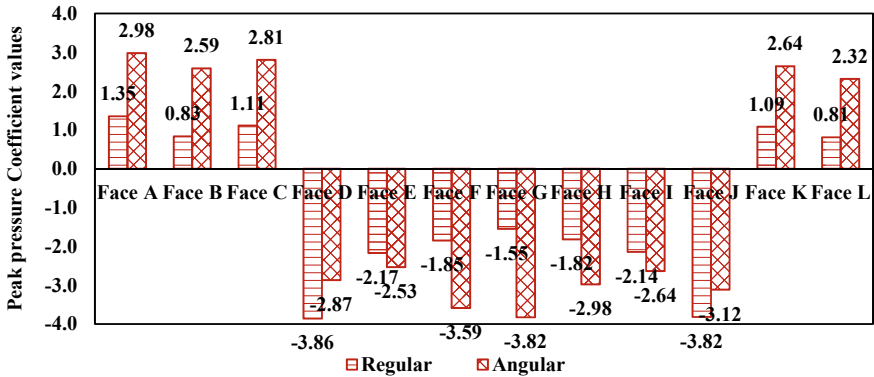
Fig. 5 Peak pressure coefficient at different surfaces (Face A to Face L) for regular and angular cross-building models at 0° wind flow

The maximum positive $\widehat{C_p}$ value is observed at Face A with a magnitude of (+)1.35 for regular cross-plan-shaped building. The critical negative $\widehat{C_p}$ value of (−)3.86 is noted at Face D for the regular building model. A much higher positive peak pressure coefficient (+)2.98 is noticed at Face A for angular building model at 0° wind flow. Face D and Face J are subjected to critical negative peak pressure coefficients due to the larger separation of flow for both building models. The negative $\widehat{C_p}$ at Face D is reduced to (−)2.87 for the angular cross-building model due to asymmetry in the building plan and lesser separation of flow. Larger difference between peak $\widehat{C_p}$ and mean C_p is noticed in the side and leeward faces for angular building model compared to regular building model (Fig. 5).

5.3 Power Spectral Density (PSD)

The power spectral density (PSD) of pressure is evaluated for all the surfaces at the height of 470 mm from the base of the building. The gauge time is considered as 3 s. Here, PSD is modified to reduced power spectral densities ($nS(n)/\sigma^2$), and frequency (n) is modified to reduced frequency (nD/U_h),

where n = frequency,
    $S(n)$ = power spectral density of pressure,
    σ = standard deviation of pressure variation with respect to time at that point,
    D = the dimension of the cross-section in the across wind direction and
    U_h = static velocity of wind at height H.

Figure 6a–l represents the PSDs plot at each surface (Face A to Face L) for both cross-plan-shaped building models for 0° wind flow direction at 470 mm height from base. The higher peak value for regular cross-plan-shaped buildings is noticed at Face A and Face B compared to the angular model. Turbulence in the flow is increased for
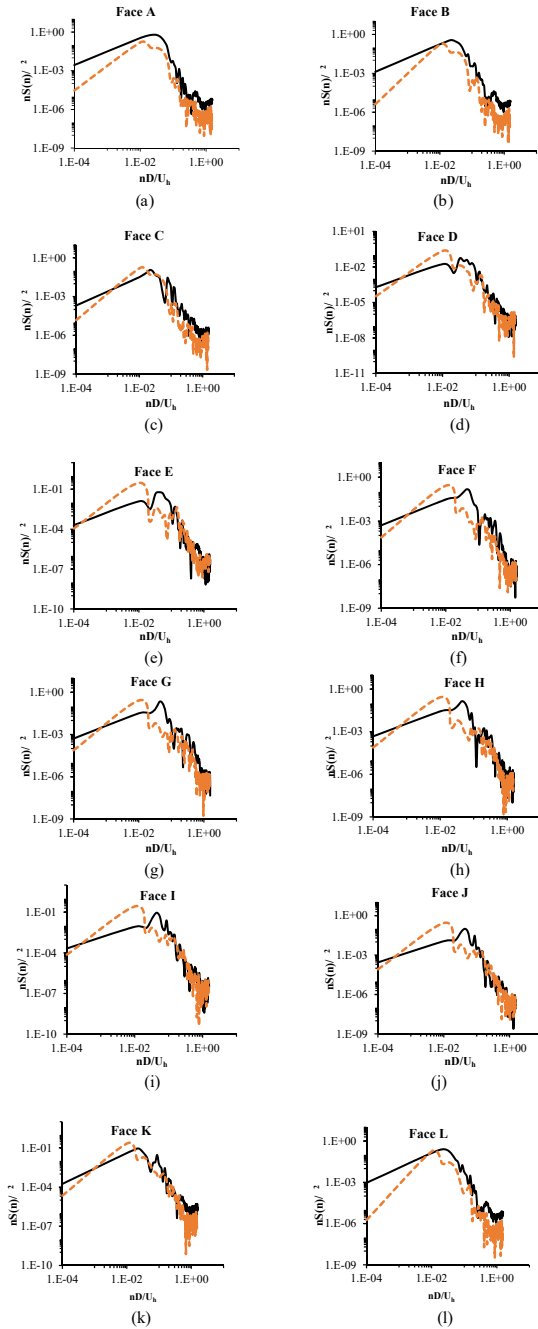
Fig. 6 The plot of reduced power spectral density with reduced frequency for regular and angular cross-plan-shaped building models at different faces for 0° wind incidence angle. **a** Face A, **b** Face B, **c** Face C, **d** Face D, **e** Face E, **f** Face F, **g** Face G, **h** Face H, **i** Face I, **j** Face J, **k** Face K, **l** Face L

the angular building model owing to the lowering of the first peak and slightly shift of peak to lower reduced frequencies. The spectral peak becomes much flat, and the spectral shape becomes much wider at Face C for angular building models, indicating vortex shedding is more random and irregular. The second peak in the PSDs pointed out the effect of strong reattachment and subsequent re-separation of the shear layer flow or flapping. Thus, the impact of mutual interference between the side faces of frontal limbs and frontal faces of the side limbs is enlightened. Being positioned on the leeward side, similar PSDs are observed for Face E to Face I for both building models. Moreover, higher turbulences on these faces are more prominent for angular cross-plan building due to gently lowering the peak and shift of peak to a slightly lower reduced frequency. Flatter spectral peak with similar spectral values is noticed for both building models at Face L.

6   Conclusions

This paper compares wind-induced responses of regular and angular cross-plan-shaped buildings through a comprehensive investigation of mean and peak pressure coefficient and power spectral densities. The numerical modelling (k-ε model) using ANSYS CFX package is used to predict the wind-induced responses for both building models at various WIA ranging from 0° to 180° at an interval of 30°. The noteworthy outcomes of the present study are summarized as follows:

- The frontal face of the frontal limb for the regular cross-plan-shaped building model is subjected to maximum mean positive pressure, which is similar to the frontal faces of regular rectangular or square plan-shaped buildings at 0° wind incidence angle. There is a reduction in the mean C_p values for angular cross-plan-shaped building at Face A for 0° wind flow conditions. The combined effect of mutual interference between the adjacent faces and being positioned on the confined region with respect to the approaching wind for 30° skew angle of flow, Face B has suffered the most critical positive mean C_p value for regular building model.
- The highest separation of wind flow leads to developing the most unfavourable mean negative Cp at the side faces of side limb (Face D and Face J) for regular cross-plan-shaped tall buildings at a critical skew angle of wind flow.
- The peak pressure coefficient for the windward face (Face A) is close to the mean pressure coefficient, while a more significant difference between peak pressure and mean pressure coefficient is noticed for the wake region (leeward and side faces) due to the high separation of flow.
- A good agreement between numerical data and experimental results indicates that numerical analysis using ANSYS CFX with k-ε turbulence model can be effectively used to evaluate wind-induced responses.
- The vortex shedding mainly influences the single peak of PSDs of Face A and Face B for regular cross-plan-shaped buildings. In contrast, the sharp second peak

is noticed for all the faces of angular cross-plan-shaped buildings, indicating both vortex shedding and the reattachment of the separated flow on the side walls.

The results obtained from numerical analysis are essential for designing a similar nature of the building. The numerical method can be an excellent weapon to handle typical irregular plan-shaped buildings.

References

1. IS:875 (Part-III) (2015) Indian standard code of practice for design loads (other than earthquake) for buildings and structures. Part 3 (wind loads). Bureau of Indian Standards, New Delhi, India
2. AS/NZS: 1170.2:2002 (2002) Structure design actions, part-2: wind actions. Australian/New Zealand Standard; Sydney and Wellington
3. ASCE: 7-10 (2010) Minimum design loads for buildings and other structures. Structural Engineering Institute of the American Society of Civil Engineering, Reston
4. Gomes MG, Rodrigues AM, Mendes P (2005) Experimental and numerical study of wind pressures on irregular-plan shapes. J Wind Eng Ind Aerodyn 93:741–756. https://doi.org/10.1016/j.jweia.2005.08.008
5. Bhattacharyya B, Dalui SK (2020) Experimental and numerical study of wind-pressure distribution on irregular-plan-shaped building. J Struct Eng 146(7):04020137. https://doi.org/10.1061/(ASCE)ST.1943-541X.0002686
6. Kumar D, Dalui SK (2017) Effect of internal angles between limbs of cross plan shaped tall building under wind load. Wind Struct 24(2):95–118. https://doi.org/10.12989/was.2017.24.2.095
7. Chakraborty S, Dalui SK, Ahuja AK (2014) Wind Load on irregular plan shaped tall building—a case study. Wind Struct 19(1):59–73. https://doi.org/10.12989/was.2014.19.1.059
8. Mukherjee S, Chakraborty S, Dalui SK, Ahuja AK (2014) Wind Induced pressure on 'Y' plan shape tall building. Wind Struct 19(5):523–540. https://doi.org/10.12989/was.2014.19.5.523
9. Pal R, Dalui SK (2016) Wind effects on 'Z' plan shaped tall building: a case study. Int J Adv Struct Eng 8:319–335. https://doi.org/10.1007/s40091-016-0134-9
10. Sanyal P, Dalui SK (2020) Effect of corner modifications on Y plan shaped tall building under wind load. Wind Struct 30(3):245–260. https://doi.org/10.12989/was.2020.30.3.245
11. Mallick M, Mohanta A, Kumar A, Patra K (2020) Gene-expression programming for the assessment of surface mean pressure coefficient on building surfaces. Build Simul 13:401–418. https://doi.org/10.1007/s12273-019-0583-8
12. Li B, Liu J, Li M (2013) Wind tunnel study on the morphological parameterization of building non-uniformity. J Wind Eng Ind Aerodyn 121:60–69
13. Li Y, Tian X, Tee KF, Li QS, Li YG (2018) Aerodynamic treatments for the reduction of wind loads on high-rise buildings. J Wind Eng Ind Aerodyn 172:107–115. https://doi.org/10.1016/j.jweia.2017.11.006
14. Liu Y, Kopp GA, Chen S (2019) Effects of plan dimensions on gust wind loads for high-rise buildings. J Wind Eng Ind Aerodyn 194:103980. https://doi.org/10.1016/j.jweia.2019.103980
15. Amin JA, Ahuja AK (2014) Characteristics of wind forces and responses of rectangular tall buildings. Int J Adv Struct Eng 6(3):1–14. https://doi.org/10.1007/s40091-014-0066-1
16. Meng F, He B, Zhu J, Zhao Amos D, Darko A, Zhao Z (2018) Sensitivity analysis of wind pressure coefficients on CAARC standard tall buildings in CFD simulations. J Build Eng 16:146–158. https://doi.org/10.1016/j.jobe.2018.01.004

17. Thordal MS, Bennetsen JC, Koss HHH (2019) Review of the practical application of CFD for the determination of wind load on high-rise buildings. J Wind Eng Ind Aerodyn 186:155–168. https://doi.org/10.1016/j.jweia.2018.12.019
18. Revuz J, Hargreaves DM, Owen JS (2012) On the domain size of steady-state CFD modeling of a tall building. Wind Struct 15(4):313–329. https://doi.org/10.12989/was.2012.15.4.313